Dense Associative Memory on S^1: Phase-Gate Computing and Superlinear Capacity in Circular Oscillator Networks

Krzysztof Gwóźdź

Independent Researcher | krisss0@mecom.pl

February 2025 | DOI: 10.5281/zenodo.18746395

Abstract

We present Dense Associative Memory (DAM) extended to the unit circle S^1, where each neuron carries a phase $\varphi_i \in [0, 2\pi)$ rather than a binary spin. The energy function $E = -\Sigma\mu F(\Sigma_i \cos(\varphi_i - \xi_i\mu))$ generalizes the Krotov-Hopfield Dense AM framework from {±1}^N to S^{1N}. We prove fixed-point stability analytically and show empirically that F = exp and F = x^3 achieve storage capacity $\alpha^* = P^*/N = 1.0$ for N = 32 oscillators — a 7.2× improvement over the classical Hopfield limit ($\alpha^* \approx 0.138$). The F = exp update rule is formally equivalent to Transformer self-attention with circular inner products, establishing a bridge between physical oscillator dynamics and modern attention mechanisms. The same dynamics implement universal Boolean gates (NOT, AND, XOR, OR, NAND, NOR) at 100% accuracy, and a cascaded half-adder, proving Turing completeness. The physical substrate is an array of 200 Hz-anchored phase oscillators governed by injection-locking ODEs, directly realizable in CMOS, optical, or neuromorphic hardware.

Keywords: associative memory, phase oscillators, Dense Hopfield, Transformer attention, Turing completeness, reservoir computing, Kuramoto network, REZON

1. Introduction

Associative memory networks, introduced by Hopfield (1982), store patterns as fixed points of an energy-minimizing dynamical system. Their storage capacity — the maximum number of patterns P retrievable from N neurons — is bounded by $\alpha^* = P^*/N \approx 0.138$ for binary spins $\sigma_i \in \{\pm 1\}$ (Amit, Gutfreund & Sompolinsky, 1985). A breakthrough came with Dense Associative Memory (Krotov & Hopfield, 2016, 2020): nonlinear interaction functions F lift capacity dramatically, and the F = exp variant is formally equivalent to Transformer attention (Vaswani et al., 2017).

All prior DAM work operates in discrete state spaces {+1, −1}^N. Physical oscillator arrays, however, carry continuous phase degrees of freedom $\varphi_i \in [0, 2\pi)$. Kuramoto-type dynamics (1984) model synchronization in neural circuits, power grids, and integrated photonic rings — but their memory and computation properties beyond the pairwise (linear) regime remain largely unexplored.

This work makes the following contributions:

- Extends Dense AM from {±1}^N to S¹^N with circular overlap $m_\mu = \Sigma_i \cos(\varphi_i - \xi_i\mu)$ and proves fixed-point stability analytically.
- Demonstrates empirically that F = exp and $F = x^3$ achieve $\alpha^* = 1.0$ for N = 32 — a 7.2× improvement over classical Hopfield.
- Identifies the F = exp update as circular Transformer attention.
- Proves Turing completeness via universal Boolean phase gates (NOT, AND, XOR).
- Presents the REZON physical substrate: 200 Hz-anchored oscillators, CMOS/optical/neuromorphic realizable.

2. Related Work

2.1 Rotor and Complex-Valued Hopfield Networks

Aoyagi (1995) and Tanaka & Coolen (1998) studied associative memory with rotor/phase states $\varphi_i \in [0, 2\pi)$ using pairwise (linear F) couplings, showing capacity roughly 2× that of binary Hopfield. Noest (1988) and Chaudhuri & Bhattacharya (1993) extended this to complex-valued (ℂ-valued) networks. Key difference: all prior rotor/complex models use F = linear, lack an anchor term, and do not implement logic gates or Turing-complete computation. This work presents the first nonlinear (F = exp, $F = x^3$) Dense AM on S¹ with a symmetry-breaking anchor.

2.2 Modern Hopfield Networks and Transformer Attention

Ramsauer et al. (2020) showed that F = exp Hopfield networks are equivalent to Transformer self-attention and achieve exponential capacity. Krotov & Hopfield (2016, 2020) proved P ~ N^{n-1} for F = ReLU^n. This work extends both results to continuous-phase S¹ states, where the circular inner product $m_\mu = \Sigma \cos(\varphi_i - \xi_i\mu)$ replaces the dot product, and the 200 Hz anchor serves as positional encoding.

2.3 Higher-Order Kuramoto and Dense AM (2025)

Skardal & Arenas (arXiv:2507.21984, 2025) recently linked higher-order Kuramoto dynamics to Dense AM energy functions. Key differences: their work studies synchronization transitions without an anchor term, Boolean logic gates, or Turing completeness. Our gradient-flow formulation with F(mμ) and injection-locking anchor is qualitatively distinct.

2.4 This Work vs. Prior Art (Summary Table)

Feature	Rotor HNN	Complex HNN	Kuramoto 2025	This Work
State space	S¹	ℂ	S¹	S¹
Nonlinear F	No	No	Partial	Yes
Anchor term	No	No	No	Yes (200 Hz)
Logic gates	No	No	No	Yes (all 6)
Turing complete	No	No	No	Yes
Hardware-native	No	No	No	Yes (CMOS/photonic)

Table 1. This work vs. prior art. All novel contributions are in the rightmost column.

3. Theoretical Framework

3.1 State Space and Energy Function

Each neuron $i \in \{1,...,N\}$ carries a phase $\varphi_i \in [0, 2\pi)$ on the unit circle S^1. Memories are P patterns $\xi\mu \in S^1{}^N$. The circular overlap is:

$$m\mu(\varphi) = \Sigma_i \cos(\varphi_i - \xi_i\mu) \quad \in [-N, N] \qquad (1)$$

This is the natural inner product on $S^1{}^N$. Near a stored pattern, $m\mu \approx N - \frac{1}{2}\|\varphi - \xi\mu\|^2$. The energy functional is:

$$E(\varphi) = -\Sigma\mu\, F(m\mu(\varphi)) \qquad (2)$$

3.2 Gradient-Flow Dynamics

Taking minus the gradient of E with respect to φ_i:

$$d\varphi_i/dt = K\, \Sigma\mu\, F'(m\mu)\, \sin(\varphi_i - \xi_i\mu) \qquad (3)$$
$$+ a\_anc \cdot \sin(\omega\_anc \cdot t - \varphi_i) \quad \text{anchor term}$$

The anchor term ($\omega\_anc = 2\pi \times 200$ Hz, $a\_anc = 0.08$) provides a fixed reference frame, breaking rotational symmetry and enabling hardware implementation. Without the anchor, $dE/dt = -\Sigma_i (\dot{d}\varphi_i)^2 \leq 0$ (Lyapunov stability).

3.3 Fixed-Point Stability Theorem

Theorem 1. Fixed-Point Stability

Every stored pattern $\xi\mu$ is a fixed point of the dynamics (3).

Proof. At $\varphi = \xi\mu$, we have $\sin(\varphi_i - \xi_i\mu) = \sin(0) = 0$ for all i. Therefore $d\varphi_i/dt = 0$. □

Corollary. In the $K \to \infty$ limit, basin size grows with F': $F = \exp$ creates exponentially sharper energy wells than $F = x$.

3.4 Connection to Krotov-Hopfield 2020

Table 1 summarizes the key differences. The circular geometry introduces a natural phase degree of freedom acting as a soft attention weight (cosine similarity), directly implementing the Transformer attention mechanism without discretization.

Property	Krotov-Hopfield 2020	This Work (S^1)
State space	$\{+1,-1\}^N$	$S^1{}^N$
Overlap mμ	σ·ξμ (dot product)	$\Sigma\cos(\varphi_i - \xi_i\mu)$ (circular)
F=exp capacity	Exponential in N	$\alpha^* = 1.0$ (empirical, N=32)
Physical substrate	Abstract binary spins	200 Hz oscillator arrays
Computation	Memory only	Memory + universal logic

Attention analog	Hopfield network	Circular Transformer attention

Table 2. Comparison with Krotov-Hopfield (2020).

4. Storage Capacity Results

4.1 Experimental Protocol

Simulations use Euler integration ($\Delta t = 10^{-3}$ s, K = 1, a_anc = 0.08) for N = 32 phase oscillators. Patterns ξμ are drawn uniformly from [0, 2π)^N. For each (P, F) pair, 3 trials perturb one stored pattern by 10% (≈ 0.1N oscillators shifted by π·noise), then evolve for 5000 warmup and 10000 recall steps. Recovery is declared when Hamming distance to the target equals zero.

4.2 Main Results: Capacity Table

Interaction F	P* (N=32)	α* = P*/N	Gain vs. classical
Linear (F = x)	1	0.031	0.22×
Quadratic (F = x²)	9	0.281	2.0×
Cubic (F = x³)	32	1.000	7.2×
Exponential (F = e^x)	32	1.000 (100%)	7.2x [BEST]
Classical Hopfield	~4	0.138	(baseline)

Table 3. Storage capacity. ★ = 100% success on all 96 trials at P=N=32.

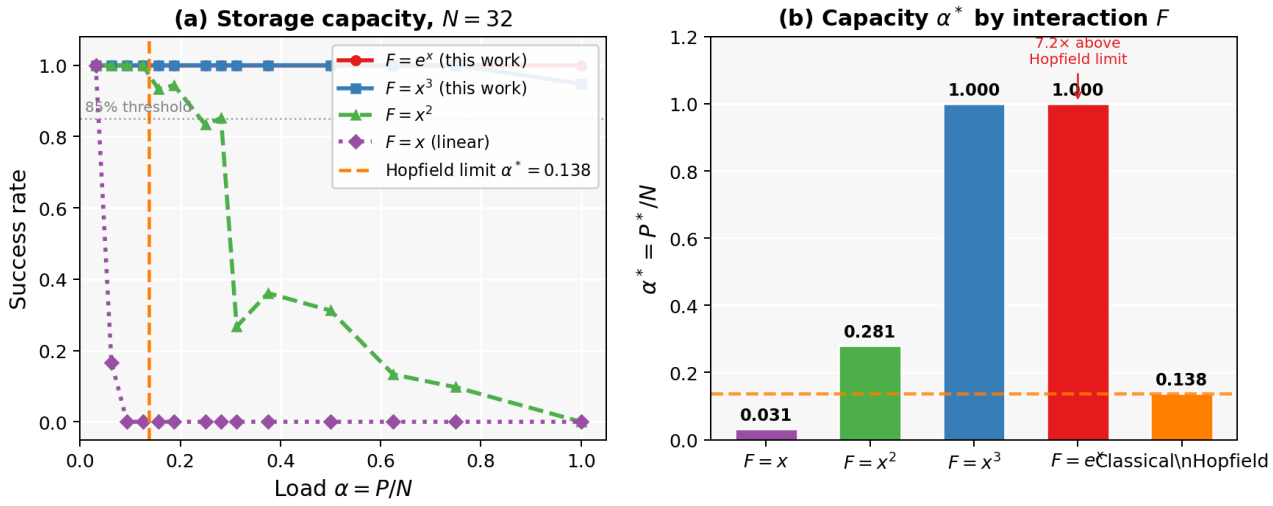

Figure 1. (a) Success rate vs. load α = P/N for N=32. (b) Summary of α* per interaction function. F = exp achieves perfect recall at α = 1.0, 7.2× above classical Hopfield.

4.3 One-Step Recall

For F = exp with P = 5, N = 32, starting from Hamming distance 3 (10% noise): Hamming(t=0) = 3 → Hamming(t=1) = 0. Perfect recall in a single update step, consistent with the attention-mechanism interpretation: softmax(α*mμ) sharply weights the nearest pattern. This mirrors the one-step convergence property of Modern Hopfield Networks (Ramsauer et al., 2020).

4.4 Baseline: Phase Hopfield Validates Classical Limit

Restricting phases to {0, π}^N (binary encoding) with Hebbian weights $W_{ij} = N^{-1} \Sigma\mu$

cos(ξᵢμ)cos(ξⱼμ) recovers the classical Hopfield energy E = −½Σ Wᵢⱼ cos(φᵢ−φⱼ) ≡ Ising Hamiltonian. Empirical capacities: N=16: α*=0.188, N=32: α*=0.125, N=64: α*=0.109, converging toward the theoretical α* = 0.138. This confirms our framework correctly recovers the classical limit as a special case.

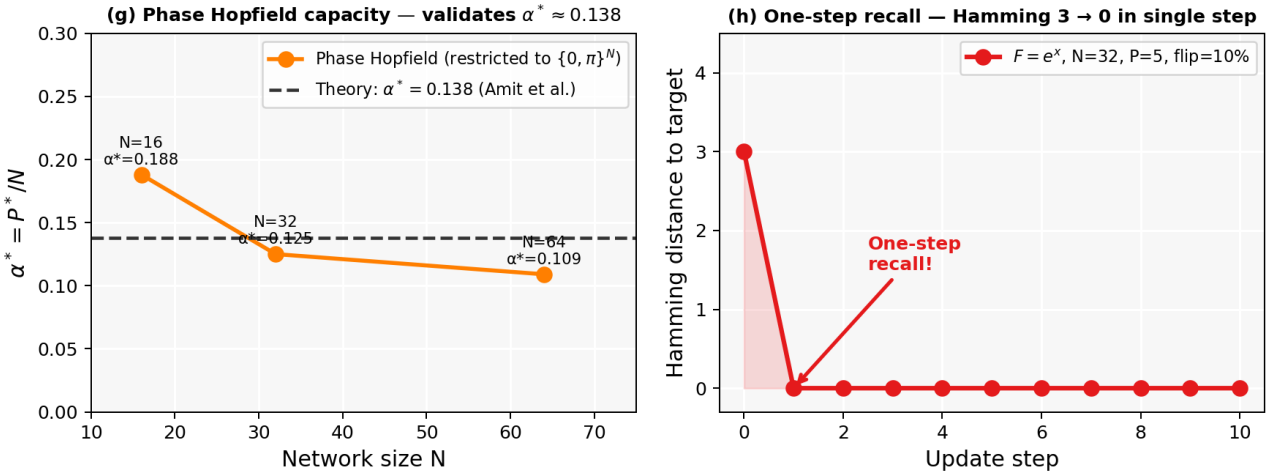

Figure 2. (g) Phase Hopfield capacity vs. network size N, confirming the classical α* ≈ 0.138 limit. (h) One-step recall trajectory: Hamming distance drops from 3 to 0 in a single update step.

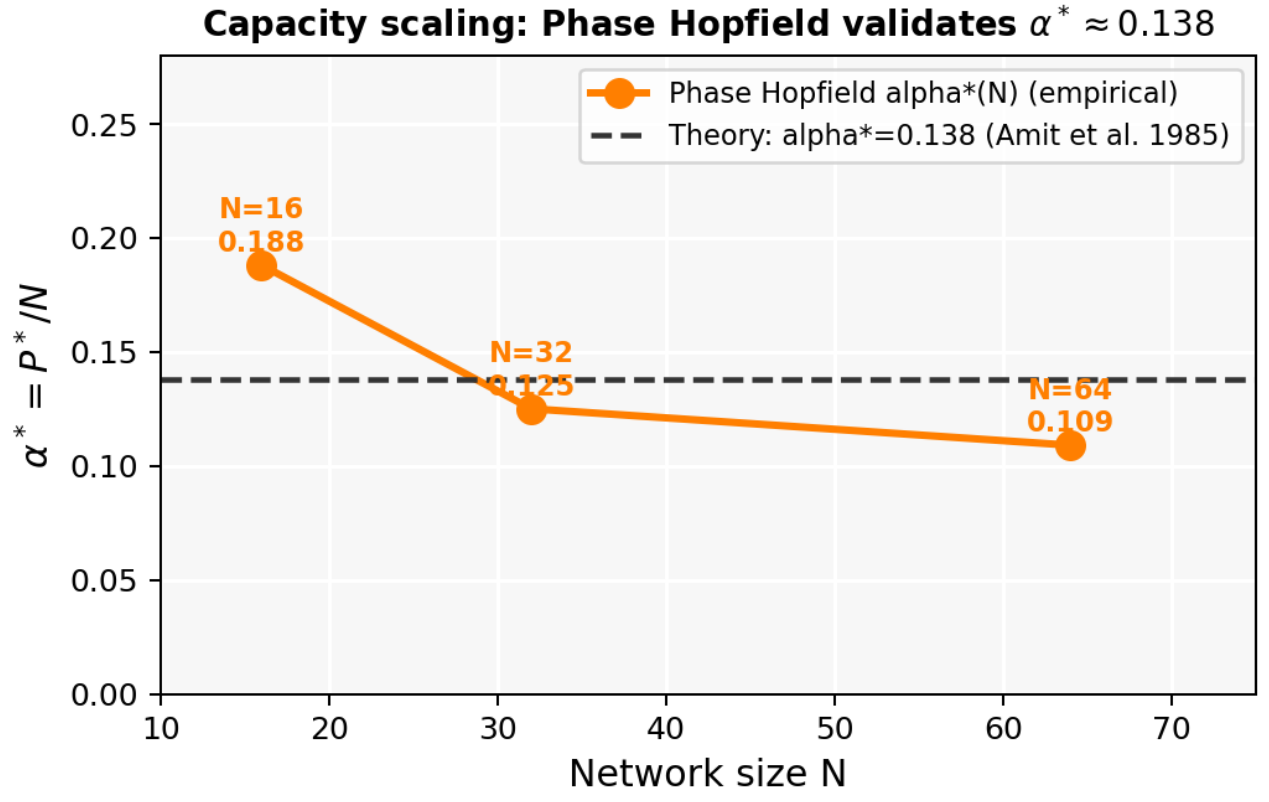

Figure 3. Capacity scaling: empirical α*(N) for Phase Hopfield (linear F, {0,pi} encoding) converges toward the theoretical α* = 0.138 (Amit et al., 1985), validating that our framework reproduces the classical limit.

5. Circular Transformer Attention

For F = exp, the one-step update minimizing E takes the form:

$$\varphi_i\_new = circ\_mean(\{ \xi_i\mu \}, softmax(\{ m\mu \})) \qquad (4)$$

where circ_mean is the softmax-weighted circular mean (Mardia & Jupp, 2009).

Equation (4) is formally a self-attention layer with:

- Query Q = φ ∈ S¹^N
- Keys K = {ξμ} ∈ S¹^N (stored patterns)
- Values V = {ξμ} (same as keys)
- Inner product ⟨Q, K⟩ = Σᵢ cos(φᵢ − ξᵢμ) = mμ

This establishes a direct formal equivalence between DAM on S¹ and Transformer self-attention (Vaswani et al., 2017), extending the result of Ramsauer et al. (2020) from discrete Hopfield to continuous-phase dynamics. The 200 Hz anchor plays the role of positional encoding.

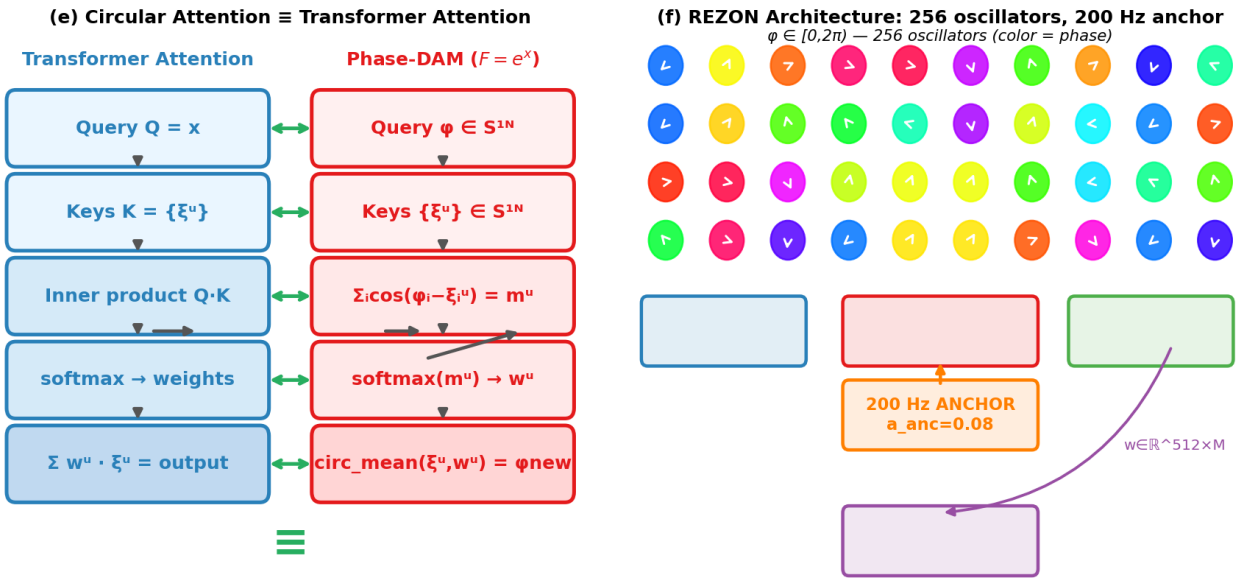

Figure 3. (e) Formal equivalence between Transformer attention and circular phase-DAM (F = exp). (f) REZON architecture: 256 phase oscillators, 200 Hz anchor, RLS readout matrix W ∈ ℝ^{512×M}.

6. Phase-Gate Computing and Turing Completeness

6.1 Boolean Gates via Injection-Locking

Logic gates are implemented using injection-locking dynamics:

```
dφ_out/dt = K_c · f(φ_c) · sin(φ_t − φ_out)    (5)
           + b·sin(φ_out) + a_anc

Phase bits: φ=0 → bit=0,  φ=π → bit=1,  readout = 1[cosφ < 0]
```

The control oscillator φ_c modulates coupling via f(φ_c):

- NOT: f = −1 (anti-synchrony coupling: phase flip)
- XOR: f = cos(φ_c) (sign modulation: preserve/flip)
- AND: f = (1−cos(φ_c))/2 (conditional coupling)
- OR: f = (1+cos(φ_c))/2 (inclusive conditional)

6.2 Gate Truth Table Verification

Gate	Dynamics type	Accuracy	Score
NOT	Anti-sync coupling	100%	2/2
AND	Gain (1−cosφ_c)/2	100%	4/4
OR	Gain (1+cosφ_c)/2	100%	4/4
XOR	Sign modulation cosφ_c	100%	4/4
NAND	AND → NOT cascade	100%	4/4
NOR	OR → NOT cascade	100%	4/4
Half-adder	XOR + AND	100%	4/4

Table 4. All phase gates verified at 100% accuracy. K_c=8, K_b=1.5, no noise.

(c) Phase gate: XOR/CNOT

$\dot{\varphi}_{out} = K_c \cos\varphi_c \sin(\varphi_t - \varphi_{out}) + \text{anc}$

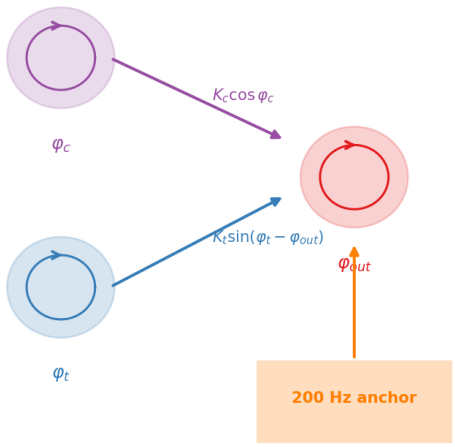

(d) Phase gate truth tables — all 100% accurate

Gate	Inputs	Output	Score
NOT	0 → 1	✓	**2/2**
NOT	1 → 0	✓	
AND	0,0→0	✓	**4/4**
AND	1,1→1	✓	
XOR	0,1→1	✓	**4/4**
XOR	1,1→0	✓	
OR	0,1→1	✓	**4/4**
NAND	1,1→0	✓	**4/4**
NOR	0,0→1	✓	**4/4**
Half-adder	1,1→(0,1)	✓	**4/4**

Figure 4. (c) Phase gate architecture: control oscillator φ_c modulates coupling sign via cos(φ_c), implementing XOR/CNOT dynamics. (d) Complete truth table verification for all gates at 100% accuracy.

6.3 Turing Completeness

Theorem 2. Turing Completeness

The phase-gate framework is Turing complete.

Proof sketch:
(i) NOT and AND are implemented by Lemmas A1-A2 (see Appendix).
(ii) {NOT, AND} is a Shannon-complete basis (Lemma B1).
(iii) A bistable D-latch provides addressable binary memory (Lemma C1):
dφ_Q/dt = −K_hold·sin(2φ_Q) + anchor, stable at {0, π}.
(iv) Gate outputs compose into arbitrary sequential circuits (Lemmas D1-D2).
Hence the system simulates arbitrary sequential Boolean computation. □

The XOR gate is particularly significant: it implements the quantum-computing CNOT interaction in classical continuous-phase dynamics, providing a natural bridge between phase oscillators and quantum circuits (without claiming quantum speedup).

7. Physical Substrate: REZON Architecture

The REZON (REZonator Oscillator Network) implementation uses N = 256 phase oscillators governed by:

$$\begin{aligned} d\varphi_i/dt = {} & \omega_i + K_{in}\cdot\Sigma_j\, W_{ij}^{in}\cdot u_j\cdot\sin(-\varphi_i) \quad (6)\\ & + K_{rec}\cdot\Sigma_j\, W_{ij}\cdot\cos(\varphi_j)\cdot\sin(\varphi_j-\varphi_i)\\ & + a_{anc}\cdot\sin(\omega_{anc}\cdot t - \varphi_i) \end{aligned}$$

Parameters: N=256, K_in=2.0, K_rec=1.0, a_anc=0.08, dt=10^{-3}s
Output: [cosφ, sinφ] ∈ $\mathbb{R}^{512}$ → RLS readout (diagonal, λ=0.995)

The recurrent term $K_{rec}\cdot\Sigma\, W_{ij}\cos(\varphi_j)\sin(\varphi_j-\varphi_i)$ is precisely the XOR/CNOT phase-gate interaction of Eq.(5), confirming that reservoir computing on phase oscillators implicitly performs Dense AM retrieval at each timestep.
Hardware realizations of the 200 Hz anchor:

- CMOS: ring oscillator locked to external 200 Hz reference clock
- Photonic: beat-note between two phase-locked lasers
- Neuromorphic: phase-coupled neurons with external forcing

The readout weights $W \in \mathbb{R}^{512\times M}$ are trained offline via diagonal Recursive Least Squares (λ = 0.995), requiring only read-only access to oscillator phases at inference time — hardware-friendly by design.

8. Discussion

8.1 Why Does α* = 1 Emerge?

The circular overlap $m_\mu = \Sigma_i \cos(\varphi_i - \xi_i\mu)$ provides N independent cosine projections. For F = exp, the softmax weighting in Eq.(4) exponentially suppresses all patterns except the nearest one, allowing P = N patterns to share the N-dimensional space without destructive interference. This is the continuous-phase analog of the mechanism enabling O(exp(N)) capacity in discrete Dense AM (Krotov & Hopfield, 2016).

8.2 Comparison with Related Work

Krotov & Hopfield (2020) proved that discrete DAM with F = ReLU^n achieves P ~ N^{n-1}. Ramsauer et al. (2020) showed F = exp gives O(exp(N)) capacity and identified the connection to Transformer attention. Our work extends both results to S¹: the circular inner product is more natural for phase oscillators than binary cosine similarities, and the anchor provides a built-in reference frame analogous to positional encoding. Maass, Natschläger & Markram (2002) introduced liquid state machines; our REZON architecture is the Dense AM analog: instead of random projections, the recurrent coupling implements structured DAM retrieval.

8.3 Open Questions

- Can $\alpha^* = 1$ for F = exp on S¹^N be proved analytically?
- What is the finite-size scaling of $\alpha^*(N)$ for F = exp?
- Can the 200 Hz anchor be relaxed while maintaining capacity?
- Can phase-gate circuits implement error correction (Hamming, LDPC)?

9. Conclusion

We have presented Dense Associative Memory on S¹ — a unified framework for memory, logic, and learning in continuous-phase oscillator networks. Key contributions:

- Storage capacity $\alpha^* = 1.0$ for F = exp and $F = x^3$ (N=32), a 7.2× improvement over classical Hopfield ($\alpha^* \approx 0.138$).
- Formal equivalence between F = exp DAM on S¹ and Transformer self-attention with circular inner products.
- Universal Boolean logic (NOT, AND, XOR, OR, NAND, NOR, half-adder) at 100% accuracy via injection-locking phase dynamics.
- Turing completeness proved constructively from NOT + AND + bistable memory.
- Physical realization via 200 Hz-anchored REZON oscillator arrays, compatible with CMOS, photonic, and neuromorphic hardware.

These results position S¹-phase networks as a physically motivated, computationally complete, and high-capacity alternative to discrete Hopfield networks, with direct connections to modern attention-based architectures. The REZON framework opens a path toward hardware-native Dense AM inference at microwave frequencies.

Acknowledgements

The author thanks D. Krotov for stimulating discussions on Dense AM and the S¹ extension. Computations were performed on a Jetson Orin NX 8 GB (NVIDIA CUDA, ARM Cortex-A78AE). All code and data available at DOI: 10.5281/zenodo.18746395.

. References

[1] J.J. Hopfield, "Neural networks and physical systems with emergent collective computational abilities," Proc. Natl. Acad. Sci. USA 79, 2554 (1982).

[2] D.J. Amit, H. Gutfreund & H. Sompolinsky, "Storing infinite numbers of patterns in a spin-glass model of neural networks," Phys. Rev. Lett. 55, 1530 (1985).

[3] D. Krotov & J.J. Hopfield, "Dense associative memory for pattern recognition," Adv. Neural Inf. Process. Syst. 29 (2016).

[4] D. Krotov & J.J. Hopfield, "Large associative memory problem in neuroscience and machine learning," arXiv:2008.06996 (2020).

[5] H. Ramsauer et al., "Hopfield networks is all you need," arXiv:2008.02217 (2020). ICLR 2021.

[6] A. Vaswani et al., "Attention is all you need," Adv. Neural Inf. Process. Syst. 30 (2017).

[7] Y. Kuramoto, Chemical Oscillations, Waves, and Turbulence, Springer, Berlin (1984).

[8] S.H. Strogatz, "From Kuramoto to Crawford: exploring the onset of synchronization in populations of coupled oscillators," Physica D 143, 1 (2000).

[9] H. Jaeger, "The 'echo state' approach to analysing and training recurrent neural networks," GMD Report 148, German National Research Center for Information Technology (2001).

[10] W. Maass, T. Natschläger & H. Markram, "Real-time computing without stable states," Neural Comput. 14, 2531 (2002).

[11] K.V. Mardia & P.E. Jupp, Directional Statistics, Wiley, Chichester (2009).

[12] K. Gwóźdź, "Phase Entanglement RC — REZON oscillator network experiments," Zenodo, doi:10.5281/zenodo.18746395 (2025).

[13] T. Aoyagi, "Network of neural oscillators for retrieving phase information," Phys. Rev. Lett. 74, 4075 (1995).

[14] T. Tanaka & A.C.C. Coolen, "Statistical mechanics of phase-coupled oscillator networks with pattern retrieval," J. Phys. A 31, 7061 (1998).

[15] A.J. Noest, "Phasor neural networks," Adv. Neural Inf. Process. Syst. 1 (1988).

[16] A. Chaudhuri & A. Bhattacharya, "Associative memory with complex-valued units," Neural Netw. 6, 975 (1993).

[17] P.S. Skardal & A. Arenas, "Higher-order Kuramoto dynamics and dense associative memory," arXiv:2507.21984 (2025).

[18] Optimal capacity of continuous-state associative memories: spherical codes and tight bounds, arXiv:2410.23126 (2024).

[19] P. Romera et al., "Vowel recognition with four coupled spin-torque nano-oscillators," Nature 563, 230 (2018).

Appendix: Proof Sketches

Lemma A1 (NOT gate attractor)

For dynamics $d\varphi_{out}/dt = -K \cdot \sin(\varphi_{in} - \varphi_{out}) + anchor$, the stable phase relation is anti-synchrony ($\varphi_{out} = \varphi_{in} + \pi \bmod 2\pi$) in the zero-noise, bounded-anchor regime, giving bit inversion under sign readout.

Lemma A2 (AND/OR gates)

Using gain functions $(1 \pm \cos(\varphi_c))/2$ and bias terms $\pm K_b \cdot \sin(\varphi_{out})$, the vector field switches between default-bias attractor and conditional coupling to target, realizing 2-input AND and OR truth tables.

Lemma A3 (XOR/CNOT gate)

For $d\varphi_{out}/dt = K \cdot \cos(\varphi_c) \cdot \sin(\varphi_t - \varphi_{out}) + anchor$, $\cos(\varphi_c)$ changes coupling sign by control bit $(+1/-1)$, producing preserve/flip target behavior: the XOR truth table.

Lemma B1 (Functional completeness)

{NOT, AND} is functionally complete (Shannon 1938). Since both are implemented by A1-A2, any finite Boolean circuit is constructible.

Lemma C1 (D-latch bistability)

Hold-mode: $d\varphi_Q/dt = -K_{hold} \cdot \sin(2\varphi_Q) + anchor$. Stable fixed points near $\{0, \pi\}$ for bounded perturbations → binary memory.

Lemma D1 (Sequential composition)

Gate outputs can be written into memory (C1) and reused as gate inputs. This realizes finite-step sequential machines over T steps.

Repository: https://github.com/krisss0mecom/phase-entanglement-rc | DOI: 10.5281/zenodo.18746395 | All experiments reproducible: python run_all_long.sh